Morphological Analysis of the Tiger Stripe on Injection Molding of Polypropylene/Ethylene-Propylene Rubber/ Talc Blends Dependent on Based Polypropylene Design

Koki Hirano,[1,2] Yoshiyuki Suetsugu,[3] Toshitaka Kanai[1,2,4]

[1]*Division of Material Sciences, Graduate School of Natural Science and Technology, Kanazawa University, Kakuma-machi, Kanazawa City, Ishikawa 920-1192, Japan*
[2]*Research and Development Division, Prime Polymer Co., Ltd., 580-30 Nagaura, Sodegaura City, Chiba 299-0265, Japan*
[3]*Central Research Laboratory, Idemitsu Kosan Co., Ltd., 1-1 Anesaki-Kaigan, Ichihara City, Chiba 299-0193, Japan*
[4]*Research and Development Laboratory, Idemitsu Kosan Co, Ltd., 1-1 Anesaki-Kaigan, Ichihara-city, Chiba 299-0193, Japan*

Received 31 March 2005; accepted 13 August 2006
DOI 10.1002/app.25393
Published online in Wiley InterScience (www.interscience.wiley.com).

ABSTRACT: Tiger stripe of injection molding of polypropylene (PP)/elastomer/talc blends was analyzed in terms of the morphology of the dispersed phase comprising elastomer components by using gloss and scanning electron microscopy (SEM). In addition, the contribution of the polymer design of PP, i.e., industrial block-type grade consisting of a homo-PP portion as the matrix and an ethylene propylene random copolymer portion as the domain is discussed. Local gloss measurement of the injected specimen along with the flow direction of the molten blends indicates a periodic fluctuation repeating higher and lower degrees of gloss, corresponding to the period of glossy and cloudy portions of the tiger stripe, respectively. These local gloss degrees are highly dependent on the morphologies of the dispersed phases near the surface layer of the injected specimen. The gloss increases when the ratio long axis (L) and diameter (D), L/D, of the dispersed phase are increased, and the gloss decreases when the L/D is decreased. Increasing the intrinsic viscosity of the ethylene-propylene rubber portion of the PP is an effective design factor for restricting the deformation against shear strain during injection process by giving the dispersed phases high elasticity. © 2007 Wiley Periodicals, Inc. J Appl Polym Sci 104: 192–199, 2007

Key words: polypropylene/elastomer/talc blend; tiger stripe; morphology, injection molding

INTRODUCTION

Polypropylene (PP) is one of the most widely used plastics in the industrial field for objects, including not only commodity equipment, packages, films, and electrical and home appliances, but automotive application as well.[1,2] PP is easily modified by blending elastomers and inorganic fillers to obtain higher performance for impact strength, rigidity, and dimensional stability, especially in automotive parts such as bumper face and instrument panel garnish. Ethylene-propylene rubber (EPR)[3–5] and talc[6] are commonly used as compounded rubber and inorganic filler, respectively. In general, injection molding method is adopted to mold these parts for its good productivity based on its relative short time spent during a molding cycle, as compared with other mold processing.

Incidentally, the striped flow mark, the so-called ''tiger stripe,'' is well known as a typical defect on the surface of injection moldings of thermoplastics. This defect is sometimes a major matter for usage of PP/EPR/talc blends, i.e., into automotive parts for which not only mechanical properties, but also industrial design, are required qualities.[7]

To obtain the high performance in impact strength and rigidity that are now required, it should be necessary to blend >20 wt % rubber and talc, respectively, to the PP/EPR/talc blends. It has been known empirically that the tiger stripe becomes worse with increasing content of both EPR and talc. Previous studies[8] have reported that both blending rubber and talc make the stripe worse. Therefore, the tiger stripe is apt to occur essentially on the injection moldings comprising the blend for the high-performance requirement in impact strength and rigidity with the addition of EPR and talc.

The tiger stripe discussed in the present study has following features: (1) striped pattern occurring down stream of the flow direction, and approximately perpendicular to the direction; (2) striped pattern consisting of

Correspondence to: K. Hirano (Koki.Hirano@primepolymer.co.jp).

Journal of Applied Polymer Science, Vol. 104, 192–199 (2007)

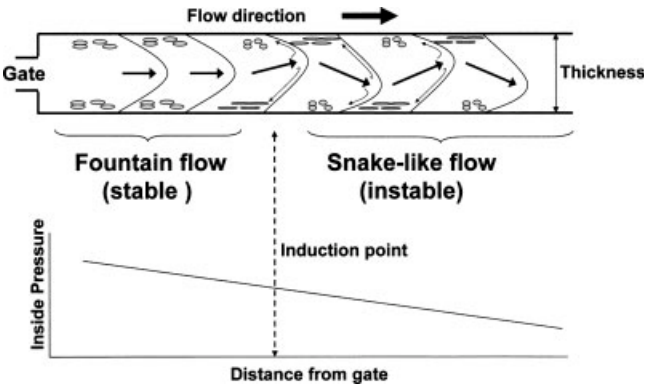

Figure 1 Schematic representations of concept for induction of tiger stripe on the basis of an unstable snake-like flow. Upper: Snake-like flow occurred at downstream with flow front fluctuation (center of fountain flow indicated by arrow). Lower: pressure loss estimated as a trigger for the unstable flow in this study.

repeating glossy and cloudy parts by naked eye observation; and (3) repeated period of the stripe is reversed on the opposite side. That is, the glossy and cloudy parts on the noted side correspond to the cloudy and glossy parts on the opposite side.

On the basis of these features, an unstable flow, referred to in the present study as the ''snake-like flow,'' model was proposed to estimate a mechanism for origin of the tiger stripe.

This model is shown in Figure 1. In this model, the molten resin flows stably at an early stage in the injecting process with the formation of a well-known fountain flow in which the flow front is symmetric in the thickness direction. However, the position of the symmetry center begins to fluctuate along the thickness direction at a given point of the latter stage. The result is a snake-like flow. The cause of the induction is not clearly understood.

Experimental observation of the stripe induction during the injection molding process was performed using visualization methods for some thermoplastic resins, for example, polystyrene (PS),[9–11] high-density polyethylene(HDPE),[9,10] PP/EPR/talc blend,[12] and polycarbonate (PC)/acrylonitrile-butadiene-styrene (ABS) blend.[13] Yokoi and Narita[12] reported that the asymmetrical fountain flow caused the induction of the tiger stripe of PP/rubber/talc blends through the visual observation by using the glass-inserted mold method. Grillet et al.[14] studied the induction of this unstable flow by using two color injection molding method and numerical analysis.

Patham et al.[15] discussed the tiger stripe of PP/ethylene α-olefin rubber blends in terms of morphology and rheology. Although these investigators discussed the effect of orientation of the rubber phase, the quantitative effect of the morphology on the stripe was not shown sufficiently.

In the present study, quantitative analysis for mechanism of the tiger stripe was performed in the morphology and polymer design of based PP, using gloss and SEM. Consequently, a model for the stripe and the design to improve its severity were proposed.

EXPERIMENTAL

Materials

To investigate the relationship between the tiger stripe and polymer designs of based PP, the homo portion of polypropylene and ethylene-propylene rubber portion were varied. It is well known that these components form a matrix and domain, respectively, in the impact-type PP.

Polypropylenes (impact-type PP containing the rubber portion) used in this study were polymerized by the Zieglar–Natta catalyst. To confirm the influence of the homo-PP portion, two series of molecular-weight distribution (MWD) were prepared: a narrow MWD and a wide MWD type having 5.5 and 11 as the ratio weight-average molecular weight to number-average one (M_w/M_n) of its homo-PP portion. J-950HP having 32 g/10 min of melt flow rate (ASTM D1238, MFR) and 13 wt % of the ethylene-propylene rubber portion (as XSP; see below) is a typical sample of the narrow MWD series, and J-985H having 25 g/10 min of MFR and 15 wt % of rubber portion is a sample for wide MWD series, respectively. Both were manufactured by Idemitsu Kosan Co., Ltd., Japan. Other PP samples used were produced by autoclaves made of stainless in laboratory scale to obtain varieties of polymer design, such as MWD and content of rubber portion (XSP) in the polypropylenes. The autoclaves used were 5 L for the narrow MWD series in the gas phase process and 2 L for both MWD series in the slurry process, respectively.

The weight fraction of ethylene propylene rubber portion was defined as a xylene soluble portion (XSP) at room temperature. The ethylene-propylene-diene-methylene rubber (EPDM) used was EP57P manufactured by JSR Co. Ltd. Japan, 88 of Mooney viscosity $ML_{1+4}(100^{\circ}C)$, 28 wt % propylene, and 15% ethylidene norbornane (ENB). The talc used was LMS-300 produced by Fuji Talc Co. Ltd., Japan.

Mixing, compounding, and injection molding process for the blends

The formulation of the blends required that the total amount of the rubber portion involving the XSP of PP and blended EPR (i.e., the total rubber component) was 30 wt %, and talc was the constant of 20 wt %. For instance, 57 wt % PP, 23 wt % EPDM, and 20 wt % of talc were mixed for the blends in which J-950HP (XSP: 13 wt %) was used before mechanical blending.

The blends were prepared using the 2FCM twin screw compounding mixer manufactured by KOBE Steel Ltd., Japan, set at 200°C of the barrel temperature, at 900 rpm of the screw speed. Productivity was 50 kg/h, 1000 ppm of antioxidant agent Irganox 1010 (Ciba Specialty Chemicals, Switzerland), and 3 parts by weight of carbon black master pellet PPM-0127 (Toyo Ink Co. Ltd., Japan) were added to 100 parts by weight of the blend to avoid thermal degradation in the process and to obtain reliable data of its tiger stripe on injected specimen by naked-eye judgment, respectively. The blends were molded using the IS200CN injection machine, manufactured by Toshiba Machine Co., Ltd., Japan, whose clamping force was 200 ton, and at an injection condition of 220°C cylinder temperature, 3.5 s injection time. The specimen shape used was a plate of 420-mm length, 100-mm width, and 3-mm thickness, having an obstacle. These specimens were exposed at trichloroethane (TCE) vapor for 60 s to remove any low-molecular-weight components from the surface before analysis.

Gloss measurement

Gloss measurement was basically performed to ASTM D523 by adopting a 5-mm square window to obtain regional gloss data at 25-mm points from the side edge. The data were measured by 5-mm steps along with the flow direction of the injected specimen of the blends.

Morphology observation and analysis

The morphology of the blends was examined with a JEOL JSM 25SIII scanning electron microscope (SEM). Sliced specimens of cross section were prepared using a glass knife and etched with 60°C xylene for 5 s to remove the rubber component, forming a dispersed phase in the blends before SEM observation. The morphology of the dispersed phase (rubber domain) was evaluated with the sizes of long axis (L) and short axis (D), and the ratio L/D used to describe the orientation of the domain. These size data were evaluated from the shape data of about 100 domains, to obtain a statistical significant difference, and average values were adopted.

Die swell measurement

The die swell ratio was measured using the Capillograph capillary rheometer manufactured by Toyo Seiki Co., Ltd., of 40-mm length and a 1-mm-diameter capillary. The strand of the molten blends was extruded through the die at 220°C in set temperature and at 1216 1/s apparent shear rate. The ratio of the diameter of the solidified strand of the blends (d_s) and the capillary diameter (d_0), d_s/d_0, were defined as the die swell ratio used in this study. The d_s/d_0 was equal to d_s, as $d_0 = 1$ mm.

RESULTS AND DISCUSSION

Quantitative evaluation of tiger stripe using the gloss measurement

Figure 2 shows a typical tiger stripe of the PP/EPR/talc blends. The severe striped pattern can easily be observed with the naked eye. This stripe was formed by alternation of a glossy (darkish) part and a cloudy (whitish) part along the flow direction in the downstream direction. It was also identified that the repeated pattern was reversed on the other surface of the specimen.

A schematic representation of the stripe is shown in Figure 3. To evaluate the stripe quantitatively, the regional gloss measurement along the flow direction was examined.

Representative data of the regional gloss profile of the blends are shown in Figure 4. A periodic fluctuation pattern repeating the top and bottom of the gloss was clearly detected. The positions of the top and the bottom data agreed with the glossy parts and cloudy parts obtained by naked-eye observation, respectively. In addition, both pitches of the gloss fluctuation and the tiger stripe also agreed. The similar results were obtained in other samples examined in this study; therefore, the pattern of the tiger stripe could be evaluated by this method.

The glossy gap ΔG was defined as the difference between the top and the bottom values of the gloss at the point 100 mm away from the end edge. In the case of Figure 4, 1.3% point of ΔG was obtained.

In the case of ΔG, less than 0.4% point, the tiger stripe was inconspicuous for naked-eye observation

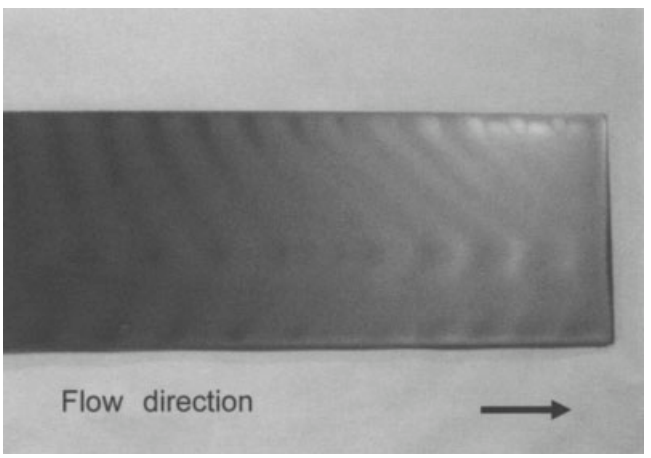

Figure 2 Typical photograph of the tiger stripe occurred on the downstream of the flow. The severe striped defect could be easily observed by naked eye. (The part near the flow end was expanded to be apt to detect by naked eye.)

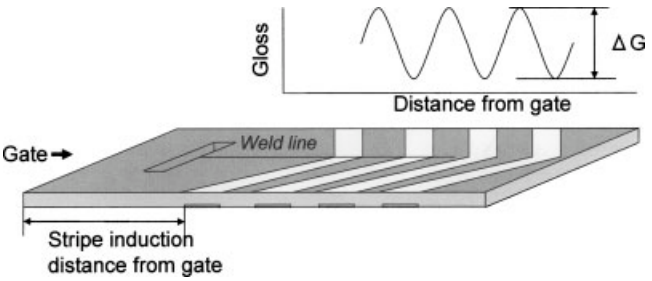

Figure 3 Schematics of tiger stripe occurring on an injected specimen of PP/EPR/talc blends. Gloss profile along the flow direction and the definition of ΔG were also shown. The obstacle size was 10 mm length and 50 mm width, and its center located on the position of 85 mm from the gate and 50 mm from the side edge.

in the author's experiment. The portions corresponding to the each gloss degree were cut out of the specimen for SEM observation.

Morphological analysis and the relationship between rubber domain and tiger stripe

The pair of SEMs in Figure 5 correspond to the representative pair of glossy and cloudy parts in the tiger stripe. Numbers of dispersed phase were observed in the photographs; however, their shape shows a clear difference between the glossy and cloudy parts. These dispersed phases could be assigned to the rubber domain comprising mixtures (i.e., the total rubber component) of the XSP of PP and blended EPR; therefore, the difference provides morphological information for the rubber domain.

It is noteworthy that the orientation of the dispersed phase was observed especially in the glossy part, rather than in the cloudy part. It is well known that shear strain during the injection molding provides the dispersed phase to be orientated along the shear flow direction, and the degree of the orientation increases with increasing shear strain. Therefore, the morphological differences in the rubbery phase indicate that a different shear strain occurred in the tiger stripe, and the glossy part was exposed in the higher strain compared with the cloudy part, although both parts were side by side in about 20 mm on the injection molding plate.

The relationship between the L/D and the regional gloss degree is shown in Figure 6. Lower and higher gloss data were observed in the lower and higher L/D region, respectively.

In the experiments performed by us, but not described in the present work, the dependence of gloss on the rubber domain orientation was evaluated in the specimen without the tiger stripe. The higher oriented rubber domain controlled by its viscosity and shear strain also provided higher gloss degree.

This relationship between gloss and rubber orientation was retained even in the tiger stripe. In the glossy part, the smooth surface having a large value in the L/D of the oriented rubber domain can reflect incident light smoothly. In contrast, in the cloudy part, the light is scattered on the rough surface having a lower value in the L/D. Therefore, the gloss degrees can be observed higher and lower for glossy and cloudy parts, respectively. Thus, it became clear that the tiger stripe recognized macroscopically by the naked eye was formed microscopically by the morphological fluctuation of the dispersed phase.

The profile of the regional gloss degree dependent on the L/D should be noted. The gradient shown in Figure 6 was gentle in the low L/D region; however, it became sharp with increased L/D of the dispersed phase.

If the snake-like flow occurred during the injection process, the dispersed phases should be exposed in the change of the shear strain along the

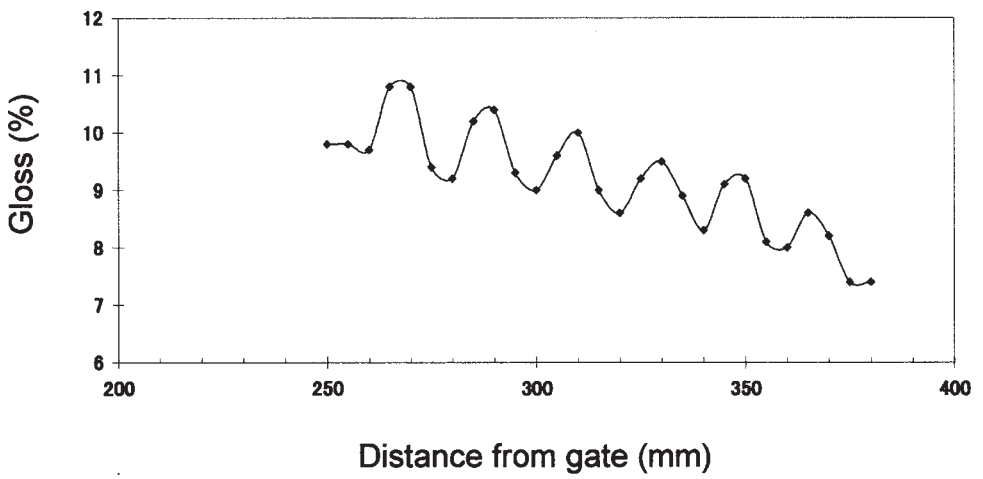

Figure 4 Regional gloss profile measured along the flow direction of a PP/EPE/talc blend used in this study. Left and right sides correspond to gate and flow end, respectively.

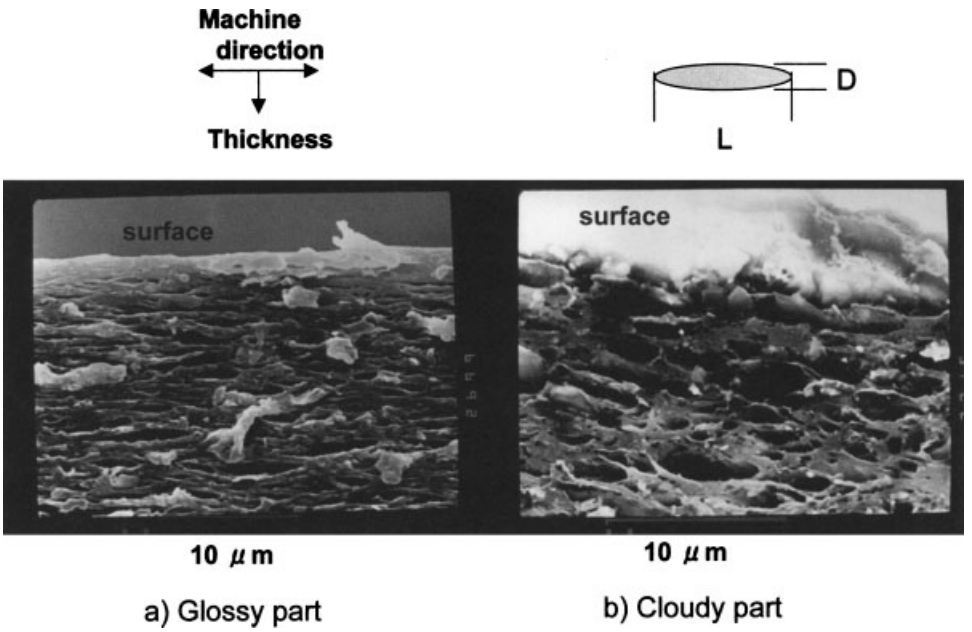

Figure 5 SEMs of morphologies of dispersed phase in depth near surface of a PP/EPR/blend used in this study; Glossy part (a) and cloudy part (b). Scale bars are 10 μm. Orientation ratio L/D is defined.

unstable flow front (Fig. 1), and then, the orientation L/D should be changed corresponding to the shear strain.

To note this morphological change of the L/D as $\Delta(L/D)$, the gloss gap ΔG is defined as the difference corresponded to the $\Delta(L/D)$ on the relationship shown in Figure 6.

As mentioned above, the severity of the tiger stripe was described with ΔG. Therefore, to reduce the severity, the ΔG should be decreased. The stripe does not appear if $\Delta G = 0$.

Figure 6 indicates the principle. The gradient k between ΔG and $\Delta(L/D)$ in Figure 6 is shown below:

$$k = \frac{\Delta G}{\Delta(L/D)} \tag{1}$$

The low value of k provides low ΔG to a given $\Delta(L/D)$ derived from the orientation change during the unstable flow, and this case can be obtained in the lower L/D region. The gloss should then be lower.

Morphology control to improve the tiger stripe by polymer design

To control the L/D, polymer designs for the based PP were discussed in terms of the viscosity ratio rubber portion as the dispersed phase and the homo-PP portion as the matrix in the blends. It is preferable ideally to adopt shear viscosity for discussion; however, the viscosity cannot be obtained easily. So the intrinsic viscosity was adopted for the index.

The intrinsic viscosity $[\eta]_{\text{total rubber}}$ is given as equation (2) due to simple addition law;

$$[\eta]_{\text{total rubber}} = \phi_{XSP}[\eta]_{XSP} + \phi_{EPR}[\eta]_{EPR} \tag{2}$$

where $[\eta]_{XSP}$ and $[\eta]_{EPR}$ are intrinsic viscosities of the xylene soluble portion (XSP) and blended EPR, respectively. In this study, $[\eta]_{XSP}$ was varied within the range of 2–7 dL/g. $[\eta]_{EPR}$ was 1.9 dL/g of the

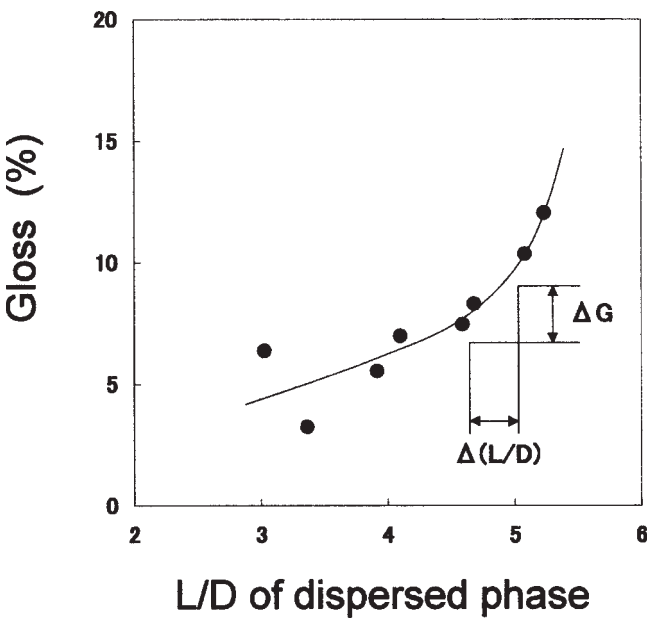

Figure 6 Relationship between regional gloss on the stripe and the L/D of dispersed phase.

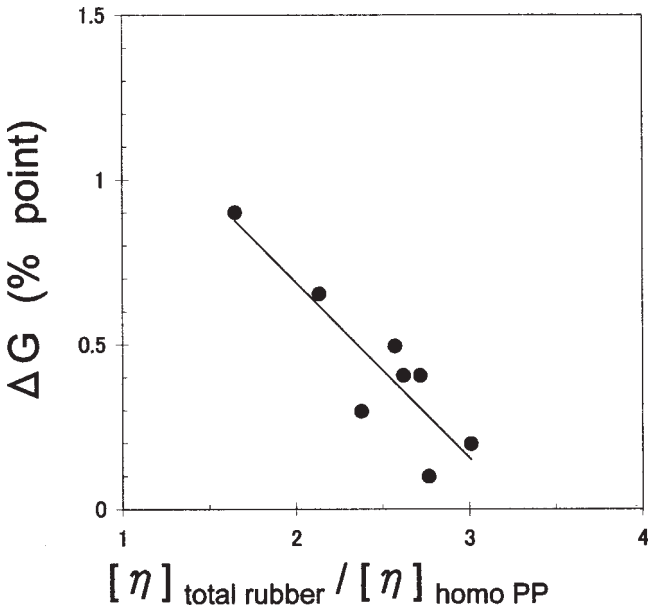

Figure 7 Relationship between gloss gap ΔG and the ratio of total rubber portion to homo-PP portion in their intrinsic viscosity.

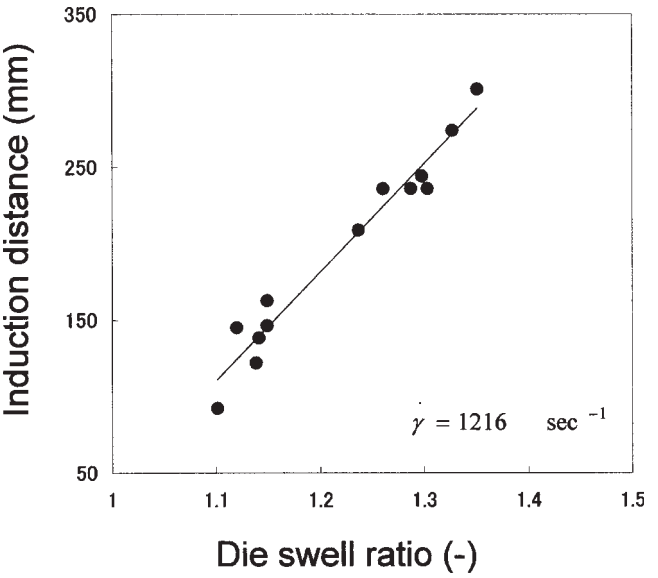

Figure 8 Relationship between induction distance of the stripe and die swelling ratio of the molten blends obtained at a given condition.

EP57P. Then ϕ_{XSP} and ϕ_{EPR} are volume fractions. Actually, the weight fraction could be adopted because of the same density 0.86 g/cm^3 for both the XSP and the EPR.

The effect of the ratio the total rubber portion and the homo-PP in intrinsic viscosity is shown in Figure 7. The intrinsic viscosity ratio $[\eta]_{\text{total rubber}}/[\eta]_{\text{homo-PP}}$ was plotted in the horizontal axis, where $[\eta]_{\text{total rubber}}$ was calculated using eq. (2), and $[\eta]_{\text{homo-PP}}$ is the intrinsic viscosity of homo-PP portion. The gloss gap ΔG clearly decreased with increasing the ratio. To obtain a lower ΔG, the ratio is required to increase by controlling polymer designs: increase in $[\eta]_{\text{total rubber}}$ and/or decrease in $[\eta]_{\text{homo-PP}}$. These polymer designs correspond to the increased dynamic viscosity ratio between the domain and the matrix consisting of a rubber portion and homo-PP portion, respectively. As a result, shear strain to the domain decreases by increasing this ratio because the domain is difficult to be deformed. Therefore, orientation (L/D) of the domain becomes lower. As mentioned above, a lower L/D gives a lower ΔG due to the relationship shown in Figure 6.

Induction distance of the tiger stripe

Some models for the induction distance of the stripe have been proposed in previous studies.[12,14,15] The authors note that the contact force of the molten blends to the mold wall is an important factor in estimating the induction mechanism.

In an early stage during the injecting process, the stable contact force performed normally to the mold wall supports the fountain flow. The elasticity of the molten blend (die swell ratio or normal stress) gives the contact force. Reduction of this force in the latter stage due to the poor elasticity of the inside pressure reduction and the molten resin having poor elasticity by nature, is apt to lose the force and to permit the snake-like flow.

The die swell ratio obtained using the capillary method was used for the index of the elasticity in this study. The MWD of the homo-PP portion and the intrinsic viscosity of XSP in the based PP controlled

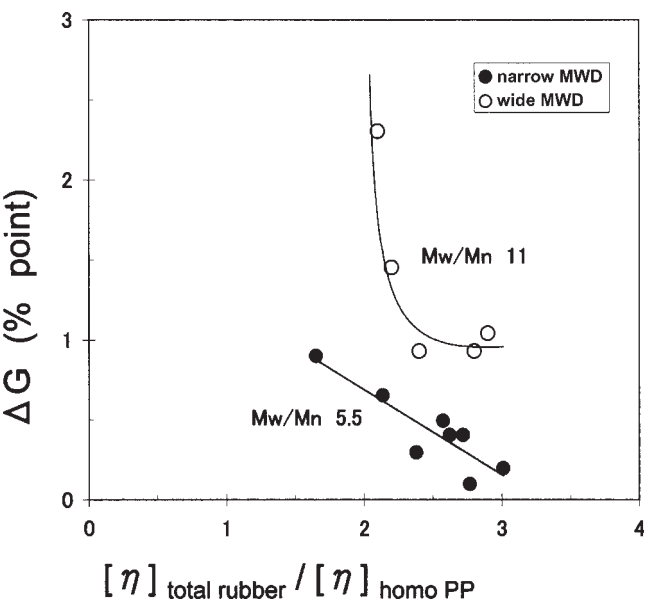

Figure 9 Effect of molecular weight distribution of homo-PP portion on the relationship between ΔG and the intrinsic viscosity ratio.

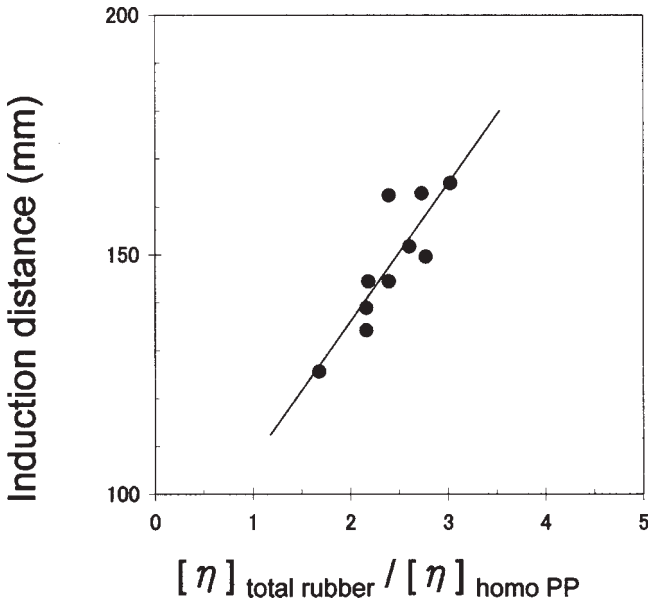

Figure 10 Relationship between the induction distance of the stripe and the intrinsic viscosity ratio the total rubber to homo-PP for the narrow MWD series.

varieties of the swell ratio. As expected, Figure 8 shows that the induction distance of the stripe increased with increased die swell ratio (d_s/d_0). It was reported that the wide MWD of the homo-PP is the method used by Fujiyama et al.[16] to obtain the large value of the die swell ratio. Remarkably, the series of wide MWD PP had both the large swell ratio and the long induction distance. These results are similar to those noted in the previous study reported by Umetani et al.[17] These investigators concluded that this result could reduce the severity of the stripe.

Although the induction distance became apart from the gate, the stripe occurred on the injection molding, even though for the wide MWD. Moreover, the severity was not adequately improved by naked-eye observation. The gloss gap for the wide MWD series dependent on the intrinsic viscosity ratio is shown in Figure 9. The profile of ΔG for the wide MWD is large compared with the profile for the narrow MWD series observed in Figure 7. In addition, the ΔG for the wide MWD series decreased until the point the intrinsic viscosity ratio of 2.4; however, the gradient was gentle for the region over 2.4 of the ratio.

Fujiyama et al.[18] reported that the thickness of the orientation zone increased with the increasing MWD of the homo-PP in injection molding.

In the case of wide MWD, the high-molecular-weight component of the homo-PP portion led to a higher orientation not only of the PP matrix, but also of the dispersed phase with forming high orientation zone in the injected specimen of the blends. The higher orientation of the dispersed phase provides a higher gloss of the glossy part in the stripe. Consequently, the ΔG increase.

The tiger stripe must occur on somewhere on the real parts for automotive applications, even if the PP/EPR/talc blends having a large value in the swell ratio are designed and the induction distance moves downstream of the injection moldings, because the real bumper required the flow length of ≥ 1000 mm from the gate to the end. Therefore, the severity of the tiger striping in the real molding should be controlled by decreasing the gloss gap. The increase in the intrinsic viscosity ratio between the rubber portion and the homo-PP increases the induction distance in the narrow MWD system (Fig. 10).

CONCLUSIONS

This study discusses the tiger stripe that occurs on the surface of injection moldings of the PP/EPR/Talc blend in its morphology and the based PP design (as shown below and summarized in Fig. 11): (a) the periodic pattern and severity of the tiger

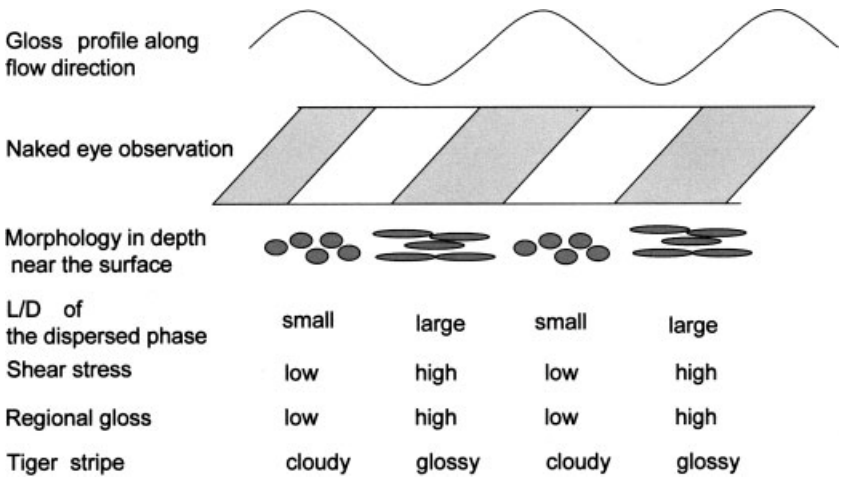

Figure 11 Schematic drawing for the tiger stripe obtained in this study.

stripe could be described using the profile of the regional gloss and the gloss gap ΔG; and (2) the regional gloss depended on the orientation of the dispersed phase comprising the rubber portion.

To improve the stripe required to decrease the gloss gap ΔG that was achieved by increasing the intrinsic viscosity ratio of the total rubber component to the homo-PP: (1) the wide molecular weight distribution of homo-PP made the stripe conspicuous and worse because of the higher orientation of the dispersed phase in the high shear zone formed during injection molding process; and (2) repeating the orientation of the dispersed phase confirmed the trace of the snake-like flow during the process.

The authors are grateful to Prime Polymer Co., Ltd., for permitting us to publish this study. Mr. Masatoshi Toda is acknowledged for kindly supplying most of the autoclave PP for this study.

References

1. Moore, E. P. Polypropylene Handbook; Hanser Gardner: Cincinnati, 1996.
2. Karger-Kocsis, J., Ed. Polypropylene: An A–Z Reference; Kluwer Academic: Dordrecht, the Netherlands, 1999.
3. Liang, J. Z.; Li, R. K. Y. J Appl Polym Sci 2002, 77, 409.
4. D'Orazio, L.; Marcarella, C.; Martuscelli, E.; Polato, F. Polymer 1991, 32, 1186.
5. van der Waal, A.; Nijihof, R.; Gaymans, R. J. Polymer 1999, 40, 6031.
6. Obata, Y.; Sumitomo, T.; Ijitsu, T.; Matsuda, M.; Nomura, T. Polym Eng Sci 2001, 41, 408.
7. Hirano, K. Idemitsu Tech Rep 2005, 48, 124.
8. Mizutani, H.; Koizumi, J.; Ito, K.; Mukai, H.; Kawashima, D. In SAE Technical Papers; Society of Automotive Engineers, 2000; paper no. 2001-1127.
9. Satoh, I.; Tredoux, L.; Kurosaki, Y. Polym Eng Sci 1999, 39, 2233.
10. Satoh, I.; Tredoux, L.; Kurosaki. Y. Polym Eng Sci 2000, 40, 2161.
11. Yokoi, H.; Motohashi, S.; Masuda, N., Seisan-Kenkyu. J Inst Indust Sci Univ Tokyo 1997, 49, 54.
12. Yokoi, H.; Narita, J. Polymer Processing Society Asia/Australia Meeting; Polymer Processing Society, 1999; p 143.
13. Hamada, H.; Tsunasawa, H. J Appl Polym Sci 1988, 60, 353.
14. Grillet, A. M.; Bogaerds, A. C. B.; Peters, G. W. M.; Baaijens, F. P. T. J Rheol 2002, 46, 651.
15. Patham, B.; Papworth, P.; Jayaraman, K.; Shu, C.; Wolkowicz, M. D. J Appl Polym Sci, 2005, 96, 423.
16. Fujiyama, M.; Kitajima, Y.; Inata, H. J Appl Polym Sci 2002, 84, 2128. 2001-1127.
17. Umetani, Y.; Matsuda, M.; Miyake, Y.; Inanami, H. In SAE Technical Papers; Society of Automotive Engineers, 2003; paper no. 2003-01-0210.
18. Fujiyama, M.; Kitajima, Y.; Inata, H. J Appl Polym Sci 2002, 84, 2142.